

# **Groundwater flow modeling and recharge stochastic analysis of the regional aquifer of the Pampa del Tamarugal–Northern Chile**

Rodrigo Rojas<sup>1</sup> and Alain Dassargues<sup>1,2</sup>

<sup>1</sup> Hydrogeology and Engineering Geology Group, Department of Geology-Geography, Katholieke Universiteit Leuven, Redingenstraat 16, 3000 Leuven, Belgium.  
[Rodrigo.RojasMujica@geo.kuleuven.be](mailto:Rodrigo.RojasMujica@geo.kuleuven.be) Phone: +32-16-326449 Fax: +32-16-326401

<sup>2</sup> Hydrogeology, Department of Georesources, Geotechnologies and Building Materials, Université de Liège, Belgium.

## **Abstract**

The *Pampa del Tamarugal* Aquifer (PTA) is an important source of groundwater in northern Chile. In this study, a groundwater flow model of this aquifer is developed and calibrated for the period 1983-2004. The model reproduces the observed flow-field and the water balance components reasonably well. Five scenarios are defined to evaluate the response to different pumping situations. These scenarios show that groundwater heads will continue to decrease with the present pumping discharge rates. To account for variations in the model results due to uncertainties in average recharge rates, randomly generated recharge realizations with different levels of uncertainty are simulated. Evaporation flow rates and groundwater flowing out of the modeled area seem invariable to the recharge uncertainty whereas the storage terms can vary considerably. For the most intensive pumping scenario under the generated random recharge rates, it is unlikely that the cumulative discharged volume from the aquifer, at the end of the simulation period, will be larger than 12% of the estimated groundwater reserve. Simulated groundwater heads fluctuations due to uncertainties in the average recharge values are more noticeable in certain areas. These fluctuations could explain unusual behavior in the observed groundwater heads in these areas.

**196 words**

**Keywords** arid regions, groundwater flow, groundwater recharge, stochastic, desierto de Atacama

## Introduction

Due to extreme arid conditions, groundwater in northern Chile is a vital resource. In the *Pampa del Tamarugal* basin (Fig. 1), annual precipitation is nil in the lower areas but reaches values of about 200 mm/yr at altitudes above 3500 m a.s.l. This spatial precipitation distribution controls the hydrology of the region. Groundwater and surface water originating in the *Andes Mountains* are the main water source for human activities (Aravena, 1995).

In this region, many coastal cities and interior towns as well as most of the mining industry entirely depend on groundwater sources. *Iquique*, the capital of the most northern region of Chile, is supplied of drinking water by means of two well fields known as *Canchones* and *El Carmelo* which are located in the *Pampa del Tamarugal* Aquifer (PTA) (Fig. 1). Due to the pumping discharge from these well fields, a steady decrease in the groundwater heads recorded in the monitoring network controlled by the *Dirección General de Aguas* (DGA) of Chile, is observed.

The study of the PTA has been a concern since the early 1960's and many local institutions and international agencies have attempted to describe the PTA, e.g., DGA. Based on a water balance at regional scale, Grilli *et al.* (1986) estimated for the DGA an average recharge flow rate for the PTA of 1002 l/s distributed over seven eastern sub-basins (Fig. 1.b). Subsequently, the DGA (1987) corrected this value to 990 l/s in the framework of a general study of the water balance of Chile.

One of the first efforts to numerically model the groundwater flow in the PTA was reported in 1988 (DGA-UChile, 1988). A groundwater flow model for steady-state conditions for the year 1960 and a transient-state modeling were developed. The model was able to reproduce the general flow-field in the area. Nevertheless, recharge coming from the most northern sub-basin (*Aroma*) was not included in this study since it was not possible to

reproduce the observed groundwater head in the northern part of the modeled area during the calibration process.

The Japanese International Cooperation Agency (JICA) jointly with the DGA and Pacific Consultants International (PCI) developed a large-scale study in the year 1995 (JICA-DGA-PCI, 1995). This study focused on the development of the water resources at a regional scale including the two most northern regions of Chile. Within the studied areas, the PTA was intensively surveyed. For this study, a groundwater flow model for steady-state conditions was developed for the year 1993. This model was able to roughly reproduce the general observed groundwater flow-field. However, two major limitations of this model can be mentioned. First, calibration process was based on unverified recharge processes where a significant amount of groundwater recharge was assumed to come from deep fissures in rock basements. This recharge mechanism was based on results that demonstrated the presence of fresh and recent groundwater at shallow levels in the centre part of the *Pampa del Tamarugal* (Margaritz *et al.*, 1990). Nevertheless, recent studies suggest that recharge at relatively shallow levels as a result of infiltrating runoff in the apex of alluvial fans originating from the eastern sub-basins is taking place (Grilli *et al.*, 1999; Houston, 2002). This certainly could also explain the presence of fresh and recent groundwater in the centre part of the PTA. Second, the assumed steady-state conditions for the year 1993 seem not valid as present time data suggest the contrary (Rojas, 2005)

Recently, Houston (2002) described the recharge mechanism in an alluvial fan located in the PTA (*Chacarilla* sub-basin). A methodology for the estimation of recharge magnitudes due to flash flood events was presented and discussed. The obtained recharge value was approximately 20% larger than the values reported in JICA-DGA-PCI (1995) for the same sub-basin.

In this context, the objective of this study is to develop an up-to-date regional-scale groundwater flow model for PTA that integrates the current knowledge and the hydrogeological information available for the region. To achieve this, a much longer period of observation data is used in the calibration process to account for transient conditions compared to previous studies. Also the most reliable and conservative estimation of the recharge is used for modeling purposes. To account for the response of the aquifer to different pumping discharge situations, a series of five scenarios are executed. In terms of predictions, simulated scenarios start from the current discharge situation (2004-2005) which allows assessing possible future strategies for management purposes. In addition, since the recharge magnitude has largely been the subject of conjecture rather than proof and calculation (Houston, 2002), another important objective which has not been included in previous studies is to account for variations in the average recharge values. To accomplish this, recharge is treated as a random variable and the model is run for a large number of stochastically generated random recharge values. In this way, the influence of the uncertainty in the groundwater recharge on the water balance components and groundwater heads in the PTA is determined. Finally, the developed model constitutes the first immediately available management tool for the DGA.

**Fig. 1**

## **Materials and Method**

### ***Study Area***

The PTA is located in the *Pampa del Tamarugal* basin within the macro-structure called *Intermediate Depression* covering an area of ca. 5000 km<sup>2</sup>. It is limited in the west by

the *Coastal Range* and in the east by the *Chilean Pre-Cordillera*. It is almost 160 km long and its width varies between 20 km and 60 km with an average elevation of 1000 m a.s.l. (Fig. 1).

Direct precipitation on PTA is nil and thus no recharge through this mechanism can be expected. On the other hand, the eastern sub-basins (Fig. 1.b) receive recharge from precipitation coming from the east and produced at high altitudes. These sub-basins lie in a well-developed rainshadow, and as a result there is a rapid decrease in rainfall as air masses move west and descend (Houston, 2002). It is also noted that in a hydrologic average year, surface watercourses disappear before reaching most of the alluvial fans located in the PTA, suggesting that part of this water is recharging the aquifer system through infiltration and lateral groundwater flows (Aravena, 1995).

The study area is part of the Atacama's desert and therefore arid conditions are extreme. According to the DGA (1987) pan evaporation rates vary between 2000 mm/yr and 2500 mm/yr. Aridity limits the presence of vegetation to very localized places in the area. These places correspond to natural or reforested areas located in the north (*Dolores*), centre (*Salar de Pintados*) and south (*Salar de Bellavista*) of the study area (Fig. 1, Fig. 4). During the 1960's, these areas were formally declared part of the *Pampa del Tamarugal Natural Forest Reserve* and from 1964 an intensive plan of reforestation started (FAO, 1989).

## **Geology**

The geology of the area has been extensively studied and described in past studies (Dingman and Galli, 1965, DGA-UChile, 1988; JICA-DGA-PCI, 1995; Digert *et al.*, 2001). As described in Houston (2002), the basin started to form in the early Oligocene and it is a complex asymmetric graben bounded in the west and in the east by N-S regional fault zones. The lowermost sediments are coarse conglomerates and gravels of the *Sichal* and *Altos de Pica Formations* eroded from the adjacent uplifted *Coastal Range* and *Pre-Cordillera*.

Throughout the Miocene, coarse clastic sediments continued to be deposited over wide areas. Some events of volcanic activity took place producing andesitic tuffs and ignimbrites from the eruptive centers located on the east. A series of large alluvial fans began to develop towards the end of the Miocene. Since the Pliocene only minor alluvial and evaporitic sediments have been deposited in the basin. The lithology of the geological units is described in Table 1.

|                |
|----------------|
| <b>Table 1</b> |
|----------------|

Fig. 2 shows a longitudinal geological profile of the study area. Basement rocks of *Longacho Formation* are differentiated in the whole area. Uplifting of this formation is observed in the north and south limits. Also in the west, in the *Coastal Range*, and in the east, outcroppings of this formation are observed. Overlying *Longacho Formation*, the *Altos de Pica Formation* differentiated in lower and upper layers, is observed. In the uppermost strata, recent sediments mainly composed of saline alluvial deposits, gravel, sand and clay have been deposited (JICA-DGA-PCI, 1995).

|               |
|---------------|
| <b>Fig. 2</b> |
|---------------|

### ***Hydrogeology***

In JICA-DGA-PCI (1995) more than 400 boring logs were interpreted and an electromagnetic survey (Transient Electromagnetic-TEM) was performed. The information from the geoelectrical profiles was complemented with the drilling of eleven wells ranging in depth between 150 m and 300 m. This analysis showed that the main aquifer system was composed of units **Q4** and **Q3**. Also in the context of this study, a series of pumping tests and

a complete re-analysis of the existing information were carried out. A summary of the aquifer parameters obtained for the PTA is presented in Table 2.

**Table 2**

DGA controls 38 observation wells in the study area (Fig. 1.c). In Fig. 3 two representative wells for the study area are depicted. Well (30) is located in the north whereas Well (72) is located in the western part of the centre zone of the study area. This last area is directly influenced by the pumping discharge of the *Canchones* and *El Carmelo* well fields. This figure shows the difference in the rate of decrease of groundwater heads for both wells.

**Fig. 3**

In Fig. 4 the equipotential map for the year 1960 is depicted from nearly 60 measurement points. The main groundwater flow direction is from north to south with an east-west component in the eastern *Pica* area. In the north area a groundwater divide is observed with part of the groundwater flowing towards the forested area in *Dolores*. Towards south, in *Huara* sector, the hydraulic gradient is considerably steep which is explained by the lower hydraulic conductivity of the deposits (DGA-UChile, 1988). In the centre, groundwater flows from east to west and flow is directed towards the western forested *Tamarugo* areas and the *Salar de Pintados*. Both correspond to the main natural discharge areas of the aquifer for the year 1960. In the southern area (*Oficina Victoria-Cerro Gordo*) groundwater flow is mainly south-west with a well defined discharge zone in the *Salar de Bellavista*.

**Fig. 4**

### ***Water Balance***

Based on DGA-UChile (1988), JICA-DGA-PCI (1995) and the record of legally constituted wells provided by the DGA, an estimation of the pumping discharge is presented in Fig. 5. In this figure, other uses are defined as: mining, industrial and irrigation discharges. The ratio (other uses/drinking water use) for the period 1961-1993 is ca. 0.2. From year 1994 onwards this ratio increases from 0.6 to 1.2 reflecting an intensive pumping discharge for other uses. This is partially explained by the very favorable results of previous studies, which resulted in an augmentation of water uses, particularly, for mining activities, and by the observed economic growth by the industrial and mining sector, specially, in northern regions of Chile.

**Fig. 5**

As previously mentioned, there is a general agreement that the recharge is mainly produced by groundwater flowing from the eastern sub-basins in the study area (DGA-UChile, 1988; JICA-DGA-PCI, 1995; Aravena, 1995; Grilli *et al.*, 1999; Houston, 2002). According to DGA-UChile (1988) there have been a series of attempts to estimate these lateral recharge flow rates. The most recent and reliable estimations of these lateral recharge (JICA-DGA-PCI, 1995) from each sub-basin are presented in Table 3.

**Table 3**

As mentioned, vegetative cover in the study area is limited to three zones: *Dolores*, *Salar de Pintados* and *Salar de Bellavista*. These zones are composed of trees highly adapted to extreme arid and saline conditions and, therefore, they can sustain themselves by absorbing



air moisture and by extracting groundwater with their massive and well developed root systems (FAO, 1989). As a consequence, it can be considered that transpiration but no evaporation occurs in these forested areas. The estimated transpiration demands are presented in Table 4.

|                |
|----------------|
| <b>Table 4</b> |
|----------------|

Another important component of the water balance is the evaporation from *Salares*. *Salares* can be defined as saline surface deposits where evaporation process can take place (Risacher *et al.* 1998). In the study area there are three *Salares*: *Salar de Pintados*, *Salar de Bellavista* and *Salar Viejo* (Fig. 4), the last one being a non-active evaporative *Salar*.

Based on data from Grilli *et al.* (1986), DGA-UCHile (1988) calculates an evaporation flow rate, jointly for *Salar de Pintados* and *Salar de Bellavista*, of 542 l/s and 286 l/s for the years 1960 and 1987, respectively. On the other hand, JICA-DGA-PCI (1995) calculates an evaporation flow rate of 145 l/s for the year 1993 also based on data from Grilli *et al.* (1986).

The groundwater flowing out in the south boundary is estimated between 164 l/s and 356 l/s (Rojas, 2005).

Results for the 1960, 1987 and 1995 water balance are shown in Table 5. For calculating the 1960 water balance, the evaporation flow rate from the *Salares* was used to close the balance assuming steady-state conditions. Recharge from the eastern sub-basins was assumed to be constant and equal to the values estimated by JICA-DGA-PCI (1995). This value was adopted since it was considered as the most reliable estimation of recharge given the longer and more recent period of analysis. Transpiration from forested areas increases due to reforestation strategies. Evaporation from the *Salares* decreases as expected due to the lowering of the groundwater heads. Groundwater flowing out of the study area was

maintained constant assuming that the main pumping discharge zone is located in the *Canchones-Pintados* area. Therefore, hydraulic gradient at the boundaries are not drastically affected by the regional cone of depression.

|                |
|----------------|
| <b>Table 5</b> |
|----------------|

### ***Groundwater Flow Model***

#### *Conceptual Model*

The model domain is limited in the west by the contact zone defined between the basement rocks of *Longacho Formation (J)* and the sedimentary materials (Fig 2). The east boundary is defined as a supposed line following roughly the main faults lineaments and the outcroppings of the *Longacho Formation*. The northern limit corresponds to *Dolores* area whereas the south limit is located southwards of the *Cerro Gordo* outcropping. This defines an area of 4303 km<sup>2</sup>, which is 160 km long and between 18 and 40 km wide. A one-layer model is assumed by combining units **Q3** and **Q4** in one hydrostratigraphic unit. This is based on the fact that most of the wells are drilled in both units and the available information on hydrogeological parameters is obtained jointly for both units. The depth of the modeled area varies between 50 m and ca. 300 m (Fig 2).

A no-flow condition is defined in the west and in the east boundaries. In the north limit, a negligible groundwater outflow is observed as mentioned in DGA-UCHile (1988) and, therefore, a no-flow condition is defined. In the south, a specified head boundary, constant in time, is defined based on observed groundwater head data. On the east, specified flux conditions are defined corresponding to the contribution of each of the seven sub-basins. This is done by incorporating point recharge wells in the apex of the alluvial fan for each of the corresponding sub-basins. No significant pumping discharge is included for the year 1960.

Evaporation and transpiration processes are also incorporated. Transpiration takes place in the *Tamarugo* areas whereas evaporation occurs in the *Salares* areas.

To implement and solve numerically the groundwater flow equation subject to the respective boundary conditions, MODFLOW (McDonald and Harbaugh, 1988) is used.

### *Model Calibration*

A two-step calibration process was performed. First, a trial-and-error calibration was done and, subsequently, the best approach reached by trial-and-error was improved using the PEST (Parameter ESTimation) algorithm (Doherty *et al.* 1994).

The steady-state model was calibrated for the year 1960. An initial spatial distribution of the hydraulic conductivity was obtained from the available data (35 measurements). Data were spatially interpolated using the kriging algorithm and the corresponding results were divided into arbitrary ranges obtaining 12 zones. During the calibration process different spatial configurations and values for the hydraulic conductivity were adopted

The transient-state model was calibrated on the period 1983-2004. For transpiration from the *Tamarugo* areas, a linear variation was assumed according to the values defined in Table 4. Parameters for calculation of the evaporation flow rates from *Salares* were maintained constant. Recharge flow rates were defined according to the values defined in Table 3. An initial spatial distribution with 4 zones was adopted for the storage coefficients based on the spatial interpolation of available data using the kriging algorithm. These values were calibrated comparing calculated groundwater heads with historical data derived from the monitoring network of the DGA. Minor adjustments to the spatial distribution of the hydraulic conductivity zones as derived for the calibration in steady-state conditions were needed.

Given the scale of the study area, calibration targets were arbitrarily defined as: Normalized Root Mean Squared (NRMS) lower than 5%, Absolute Residual Mean (ARM) lower than 1.5 m, Root Mean Squared (RMS) lower than 2 m.

### *Simulation Scenarios*

The model was run for four future scenarios of groundwater consumption in the PTA. In the fifth scenario, recharge was treated as a random variable and the model was run for a large number of stochastically generated random recharge values. Initial conditions were obtained from the last year (2004) in the transient calibration. The simulated period corresponds to 2005-2050.

*Scenario 2005*: pumping discharge situation of the year 2004-2005 (1585 l/s = 871 l/s for other uses + 714 l/s for drinking water requirements).

*Scenario 2005 + 20%*: pumping discharge situation of the year 2004-2005 increased by 20% (1900 l/s).

*Scenario 2005 – 20%*: pumping discharge situation of the year 2004-2005 decreased by 20% (1268 l/s).

*Scenario Drinking Water Projection (DWP)*: This scenario corresponds to the projection of the drinking water demands for the city of Iquique. In this scenario the pumping discharges for drinking water purposes were linearly projected from 714 l/s up to 1235 l/s whereas the other uses demands were maintained constant to the 2005 situation (871 l/s). Thus, the final pumping discharge for the 2050 year totalized 2106 l/s. This water demand for drinking water purposes was estimated based on the projection of population and the corresponding water requirements (JICA-DGA-PCI, 1995; Arrau, 1998; Brown 2003; Rojas, 2005). It was also assumed that drinking water for Iquique city would be largely extracted from the PTA with the pumping infrastructure of the year 2005.

*Scenario DWP + Randomly Generated Recharge*: Based on the scenario *DWP*, the effects of different average recharge flow rates on groundwater heads and flow components of the water balance were analyzed. Series of 100 purely random realizations of average recharge values were generated for three levels of uncertainty expressed as a percentage of the average recharge ( $R$ ) values presented in Table 3. The level of uncertainty was set arbitrarily in  $\sigma_1=0.05R$ ,  $\sigma_2=0.15R$  and  $\sigma_3=0.35R$ . Random recharge flow rates were generated for each sub-basin using a random number generator honoring a log-normal distribution to avoid negative values. Spatio-temporal structure of correlation for the recharge values were not considered in the synthetic generation.

## Results

### *Steady-state and transient-state calibration*

The calibrated values for hydraulic conductivities (24 zones) vary between  $3 \times 10^{-2}$  m/d and  $6.7 \times 10^1$  m/d with a geometric mean  $K_{GM} = 3.5$  m/d. The observed vs. simulated groundwater heads for year 1960 are shown in Fig.6.a. For the transient-state calibration, a final set of 10 zones for the storage coefficient ranging from  $5 \times 10^{-3}$  up to  $3 \times 10^{-1}$  is obtained. The observed vs. simulated groundwater heads for the period 1983-2004 are shown in Fig. 6.b. These values are considered satisfactory based on the calibration targets.

**Fig. 6**

The spatial distribution of the errors terms is depicted in Fig. 7. Simulated groundwater heads are clearly overestimating the observed values in the middle of the domain (*Canchones-Pintados*) where head residuals are in the order of 2 m up to 4 m. In the west of

the domain, observed values are underestimated in the order of 1 m up to 2 m. In the north of the model area, the residuals are in the order of 1 m.

**Fig. 7**

The simulated water balance for years 1960, 1987 and 1993 is presented in Table 6. All flow terms are in agreement with estimations made in Table 5. Some minor discrepancies are observed in the transpiration term from *Tamarugo* areas which are derived from the interpolation of the values of Table 4. Groundwater outflows from the modeled area are nearly constant around 160 l/s for the whole period (1960 and 1983-2004). Although the trend of decreasing in evaporation flow rates from the *Salares* is confirmed, simulated values are overestimating estimations of table 5. This difference can be explained by the generalized overestimation of groundwater heads in the sector of *Salar de Pintados* and the uncertainty in the definition of the active evaporative surface of the *Salares*.

**Table 6**

In Fig. 8 some representative wells of the study area are presented. The overall trend of groundwater head decrease is reasonably well simulated in the north area (*Well Dolores* - Fig. 8.a) and in the centre-north area (*Well 60-59* - Fig. 8.b). However, short-term variations are not reproduced by the model.

**Fig. 8**

In *Well 134* (Fig. 8.c), located in the centre area of the model domain (*Canchones*), the overall tendency of decrease is fairly modeled until the beginning of the year 1999. After that, a significant increase in the groundwater heads is observed, which is also properly simulated. This reflects the effect of *Canchones* well field being replaced during the period 1998-1999 by the *El Carmelo* well field. This is also noticed in observation *Well 60-59* (Fig. 8.b), located near *El Carmelo* well field, which shows a change in the slope of the overall trend for that year. In the centre-south area (*Well 31*), observed values are clearly overestimated and the trend in groundwater heads is not properly simulated (Fig. 8.d). In general, this area presents an overestimation of the observed heads for a large number of observation wells. This is indicating that the extension of the cone of depression produced by the *Canchones* well field is not properly reproduced towards south-west areas in the middle of the model domain.

In the south area (*Well 276*) the modeled results are in concordance with the overall trend (Fig. 8.e). Differences between simulated and observed groundwater heads are smaller than 1.5m.

### ***Sensitivity Analysis***

A sensitivity analysis was performed for the following calibrated parameters: constant head at the south boundary condition (SBC), evaporation rate, extinction depth for the evaporation process, recharge flow rates and hydraulic conductivities.

The applied head at the SBC was varied between 20 m below and above the calibrated value. The performance of the model in terms of the calibration targets was stable up to  $SBC \pm 10$  m. For values greater than  $SBC+10$  m, the groundwater head increased in such a way that evaporation took place in the *Salar Viejo* which, based on field observations, is unrealistic.

Evaporation rate and extinction depth were varied between 1250 mm/yr and 2500 mm/yr, and 0.2 m and 1.8 m, respectively. In terms of calibration targets and flow components, results were insensitive to changes on both of these parameters.

For the recharge flow rates an arbitrary range of variation was selected ( $R \pm 0.5R$ ). NRMS, RMS and ARM were rather sensitive to changes in recharge rates. Evaporation in the *Salar de Pintados* was the most sensitive flow component with a 50% increase in recharge producing an 80% increase in evaporation.

Each of the 24 calibrated hydraulic conductivity zones was multiplied by the following factors: 0.01K, 0.1K, 0.5K, 5K, 10K and 100K. Changes in the spatial configuration or combined sensitivity of two or more K-parameters were not evaluated. Model results were particularly sensitive to changes in the hydraulic conductivity in *Pintados-Canchones* area since most of the wells are located in that area. In terms of flow components, a variation from 0.5K up to 10K resulted in groundwater outflows through the SBC contained in the defined range (164 l/s - 356 l/s). For the evaporation flow rate, a variation between 0.1K up to K resulted in evaporation flow rates in the estimated range (410 l/s - 602 l/s).

## ***Results simulation scenarios***

### *Water Balance results*

Fig. 9 shows the simulated flow components of the PTA for different scenarios in an annual basis. In Fig. 9.a evaporation flow rates for different scenarios are depicted. The variations between scenarios *2005*, *2005 + 20%* and *DWP* are negligible. However, for scenario *2005 - 20%* evaporation flow rates are slightly larger suggesting that actual pumping discharge is consuming groundwater that otherwise would be lost through evaporation. This is quite reasonable since most of the production wells are not located near *Salares* area and,



therefore, any increase in pumping discharge is partially not reflected in evaporation flow rates decreases.

**Fig. 9**

Figure 9.b shows the annual groundwater flow to storage. The peak produced in the groundwater flow to storage during the year 1998-1999 is explained by the cease of the pumping discharge from the *Canchones* well field. This cease of pumping induced a considerable recovery of the groundwater heads (Fig. 8.c). After year 2005 groundwater going to storage for scenarios *2005*, *2005+20%* and *2005-20%* decreases to zero value between years 2020 and 2030. Scenario *DWP* accelerates the depletion of this component reaching zero value by year 2013. This is explained by the fact that when drinking water demands exceed the *El Carmelo* well field pumping capacity, *Canchones* well field capacity is used. Fig. 9.c shows loss of groundwater storage, i.e., groundwater storage entering the “mobile” flow system to supply the demand. For scenarios *2005*, *2005 + 20%* and *2005 – 20%* this component smoothly decreases and remains roughly constant after year 2040. On contrary, for scenario *DWP* the increase in the loss of groundwater storage is due to the increase in pumping discharge as response to increasing groundwater demands for drinking water purposes.

In the case of *DWP* scenario under random recharge flow rates, main results are presented in Fig. 10. Changes in the evaporation flow rates and groundwater flowing out of the modeled area are imperceptibles for  $\sigma_1$ ,  $\sigma_2$  and  $\sigma_3$ .

Results for the loss of groundwater storage under random recharge flow rates for  $\sigma_3$  and 100 recharge realizations are shown in Fig. 10.a. In this figure, the black line represents the scenario *DWP* under average recharge flow rates (976 l/s).

**Fig. 10**

Fluctuations of the average and standard deviation of the loss of groundwater storage, for the last year of simulation (2050) vs. number of realization, are shown in Fig. 10.b and 10.c, respectively. From these figures, tendencies are clearly seen and for  $\sigma_1$ ,  $\sigma_2$  and  $\sigma_3$  the loss of groundwater storage is in the order of  $2060 \text{ l/s} \pm 23 \text{ l/s}$ ,  $2085 \text{ l/s} \pm 65 \text{ l/s}$  and  $2100 \text{ l/s} \pm 110 \text{ l/s}$ , respectively.

On the other hand, for  $\sigma_1$ ,  $\sigma_2$  and  $\sigma_3$ , the cumulative loss of groundwater storage for the last year of the simulation period (2005-2050) was obtained for each recharge realization. From these results, three probability distributions were obtained for the cumulative loss of groundwater storage at year 2050. In Fig. 10.d the probability distribution of the cumulative loss of groundwater storage for  $\sigma_3$  is depicted. Based on the estimated groundwater storage reserve made in JICA-DGA-PCI (1995) for PTA ( $26.9 \times 10^9 \text{ m}^3$ ) and from figure 10.d, it is unlikely that the cumulative loss of storage for supplying the demand of the system in the year 2050 will be larger than 12% of the estimated groundwater storage reserves.

#### *Groundwater heads*

In the north sector, none of the wells seems to present large impact on the groundwater heads for the different scenarios. For the centre-north sector, the largest decrease in groundwater heads is produced by scenario *2005+20%*. By the end of the simulation period, the drawdown is in the order of 2 m in comparison to scenario *2005*. On the other hand, in the centre-sector near *Canchones* well field, the largest drawdown is produced by scenario *DWP* (ca. 18 m) whereas for *El Carmelo* well field the largest drawdown is 3 m. For the south sector, no major effect on groundwater heads for scenarios *2005+20%* and *DWP* in comparison to scenario *2005* are observed.

To assess the effect of random recharge rates on the simulated groundwater heads, seven artificial observation wells are located at different representative places. For an observation well located in the lower area of the alluvial fan produced by the *Aroma* creek (north), fluctuations (for  $\sigma_1$ ,  $\sigma_2$  and  $\sigma_3$ ) in groundwater heads are between 0 m and 1.5 m (Fig. 11). For observation wells located in the lower part of the alluvial fan of *Tarapaca* and *Sagasca* creeks (north and centre), significant groundwater heads fluctuations are observed only for  $\sigma_3$  and they are in the order of 0.4 m - 1 m at the end of the simulated period. These areas present the largest variation from the average recharge situation. This could be explained because they are located in the confluence of *Aroma* and *Tarapaca* sub-basins, which jointly generate ca. 50 % of the total incoming groundwater recharge.

**Fig. 11**

Observation wells located in the centre areas present minor fluctuations (0.1 m) for the largest uncertainty level ( $\sigma_3$ ). For an observation well located in the alluvial fan of *Chacarilla* creek (south), fluctuations from the average recharge situation are in the order of 0.5 m.

From this, it is clear that the northern *Aroma* and *Tarapaca* sub-basins influence the groundwater heads in the north sector of the study area. If the groundwater recharge coming from these sub-basins changes in magnitude, it will be reflected in areas as far as 19 km from *Aroma* alluvial fan apex or 15 km from *Tarapaca* alluvial fan Apex. Also the southern *Chacarilla* sub-basin has minor influence on the groundwater heads located in the lower areas of the corresponding alluvial fan.

## Discussion and Conclusions

PTA is a strategic source of groundwater which is intensively used since 1960's. The groundwater extraction for different purposes has a clear effect on the observed groundwater heads, especially, in those zones affected by the *Canchones* and *El Carmelo* well fields. In these areas a more pronounced drawdown is observed compared to other areas. Although Houston (2002) suggested that these long-term drawdowns in groundwater heads may partly result from long-term climatic fluctuations, it is likely that these drawdowns are simply due to overexploitation.

This study develops an up-to-date groundwater flow model, calibrated for steady-state conditions (1960) and transient-state conditions (1983-2004). Different groundwater extraction situations are considered and, more important, a sensitivity study to the average recharge values is performed. Calibration criteria defines an acceptable performance of the model with final calibrated parameters contained in realistic ranges which do not substantially differs from values obtained in past studies. Also groundwater balance results are in agreement with previous estimations made in past studies.

The impossibility to estimate pumping discharges at a time scale less than one year without an exhaustive field-work, make not possible to reproduce short-term fluctuations in the observed groundwater heads, particularly, in those wells affected by local pumping conditions.

The observed overall trend of the groundwater heads and the observed flow-field are properly reproduced with the exception of a limited area towards *Salar de Pintados*.

Related to the water balance components, simulated evaporation flow rates overestimate calculations made in past studies. This can be attributed to two main factors: first, the simulated groundwater heads overestimate the observed groundwater heads in the *Salar de Pintados* area and, second, the uncertainty in the actual extension of the surface

where evaporation process from *Salares* takes place. These two points represent the major limitations of the groundwater flow model. To alleviate these limitations it is suggested to fully describe in a three dimensional conceptual model this area and to define in a more accurate way the active surface for evaporation process.

Scenarios show that groundwater heads will continue to decrease with the actual pumping discharge (2005). This decrease is slightly more severe for an increase of 20% in the artificial discharge. For the case of *DWP* scenario, areas located near *Canchones* well field are more drastically affected than areas located near *El Carmelo* well field. Although this is strictly related with the assumptions that defined the respective scenarios, even a reduction in the actual pumping discharges shows this trend of increasing drawdowns. It is clear that in the mid and long-term, groundwater users of PTA will be facing a worst situation than the present one.

On contrary, if pumping discharges are reduced, the evaporation flow rates tend to slightly increase suggesting that part of the present system demand is supplied by groundwater consumed by the evaporation process. This confronts two viewpoints: to reduce the present pumping discharge to reduce the demand on the system, knowing that part of this reduced discharge will be lost through evaporation from *Salares*, or to increase the actual pumping discharge to the point where no groundwater is lost through evaporation.

For scenario *DWP* under random recharge values, evaporation flow rates from *Salares* and SBC groundwater outflows are invariable to all uncertainty levels in recharge ( $\sigma_1$ ,  $\sigma_2$  and  $\sigma_3$ ). This could be related to the time span (45 years) used to evaluate the flow components under random recharge values, which could suggest that the simulation period might be too short to observe more pronounced effects.

In terms of storage flow components, they vary according to the level of uncertainty. The loss of groundwater storage for supplying the system demand increases when the

uncertainty in the recharge increases. Despite of this, the cumulative loss of groundwater storage represents less than 12% of the assessed groundwater total reserves.

Uncertainties in the simulated groundwater heads due to uncertainties in average recharge rates are more noticed in areas near *Aroma*, *Tarapaca* and *Chacarilla* creeks. These sub-basins represent ca. 81% of the total incoming recharge. Although these fluctuations in groundwater heads are minors, they certainly could explain observed unusual behavior in wells located in these areas, where some local recharge events could be expected.

Finally, it is clear that temporal and spatial variation of the recharge events may play an important role. The use of a stochastic framework in the groundwater modeling has demonstrated this fact, especially, in those zones where the random nature, spatial and temporal, of the precipitation (assuming it as the main source of groundwater recharge) is much more pronounced, e.g., arid zones. Undoubtedly, the northern part of Chile is one of these zones and similar approaches can be extended to other aquifers in similar arid zones.

### **Acknowledgements**

The authors wish to thank to the Dirección General de Aguas – Chile for providing all the necessary data for the development of this study.

### **References**

Aravena R (1995) Isotope hydrology and geochemistry of northern Chile groundwaters. Bulletin de l'institute français d'études andines, 24 (3):495-503

Arrau F (1998) Distribución y comercialización de las aguas en Chile [Water distribution and commercialization in Chile]. Chile Congress Library. Study Series No 178.

Brown E (2003) Uso eficiente del recurso hídrico [Efficient use of the water resource]. In: National Workshop – Chile Towards a national plan of integrated water resources management CEPAL – Chile. December 2003. 22 pp.

Doherty J, L Brebber, P Whyte (1994) PEST: Model-independent parameter estimation. User's manual. Watermark Computing.

Digert F; Hoke G; Jordan T; Isacks B (2001) Subsurface stratigraphy of the neogene Pampa del Tamarugal basin, northern Chile. XI Geological Congress Chile. 8 pp.

Dingman R; Galli C (1965) Geology and groundwater resources of the Pica area, Tarapaca Province, Chile. Bulletin of the United States Geological Survey No 1189.

Dirección General de Aguas – DGA (1987) Balance hídrico de Chile [Water balance of Chile]. Technical Report – Digital data.

Dirección General de Aguas – Universidad de Chile DGA-UChile (1988) Modelo de simulación hidrogeológico de la Pampa del Tamarugal [Hydrogeological simulation model of the Pampa del Tamarugal]. Technical Report, 98 pp.

Food and Agriculture Organization – FAO (1989) Role of Forestry in combating desertification. FAO Conservation Guide 21.

Grilli A; Vidal F; Garín C (1986) Balance hidrológico nacional, I Región [National hydrologic balance, I Region]. Dirección General de Aguas. Technical Report EH/86/2.

Grilli A; Aguirre E; Duran M; Townsend F; Gonzales A (1999) Origen de las aguas subterráneas del sector Pica-Salar del Huasco, Provincia de Iquique, I Región de Tarapaca [Origin of the groundwater in the sector of Pica-Salar del Huasco, Province of Iquique, I Region of Tarapacá]. In: AIDIS-CHILE Congress. 18 pp.

Houston J (2002) Groundwater recharge through an alluvial fan in the Atacama Desert, northern Chile: mechanisms, magnitudes and causes. Hydrological Processes, 16: 3019-3035.

Japanese International Cooperation Agency JICA; Dirección General de Aguas DGA; Pacific Consultants International PCI – JICA-DGA-PCI (1995) The study on the development of Water Resources in northern Chile. Technical reports. Supporting reports B and C. 259 pp.

Margaritz M; Aravena R; Peña H; Suzuki O; Grilli A (1990) Source of groundwaters in the deserts of northern Chile: evidence for deep circulation of groundwaters from the Andes. *Ground Water*, 28: 523 – 517.

McDonald M, Harbaugh A (1988) A modular three-dimensional finite-difference groundwater flow model. USGS Technical Report on Modelling Techniques Book 6. 596 pp.

Risacher F; Alonso H; Salazar C (1998) Geoquímica de aguas en cuencas cerradas I, II y III regiones – Chile [Water geochemistry in closed basins I, II and III regions – Chile]. Technical Report DGA-UCN-ORSTOM. 84 pp.

Rojas R (2005) Groundwater flow model of Pampa del Tamarugal Aquifer – Northern Chile. MSc Thesis Water Resources Engineering. Catholic University of Leuven and Free University of Brussels. 103 pp.



Table 1: Stratigraphic classification and lithology description (after JICA-DGA-PCI, 1995)

| Geologic Age | Formation               | Lithology  | Units       |    |
|--------------|-------------------------|--|-------------|----|
| Quaternary   | Recent Sediments        | Alluvial, Eolian, Fan deposits: Saline alluvial deposits; Clay, sand and gravel; gravel, sand and clay.                                    | Qal, Qe, Qf | Q4 |
|              | Altos de Pica Formation | Continental and sedimentary rocks.   | TQau        | Q4 |
|              |                         | <i>Member 5</i> : Middle sandstone (200 m thickness). Sandstone and conglomerate.  |             | Q3 |
|              |                         | <i>Member 4</i> : Rhyolitic tuff (23 m thickness). Andesitic to dacitic ignimbrite.  |             | Q2 |
|              |                         | <i>Member 3</i> : Middle to coarse sandstone (173 m thickness). Sandstone with conglomerates.  |             |    |
| Tertiary     |                         | <i>Member 2</i> : Rhyolitic welded tuff (17 m thickness). Andesitic ignimbrites and tuffs  | TQal        | Q1 |
|              |                         | <i>Member 1</i> : Conglomerate and middle to coarse sandstone (322 m thickness).   |             |    |
| Mesozoic     | Longacho Formation      | Fissible shale, mudstone, fine sandstone, limestone. This formation is intruded by andesite, dacite, diorite, granite, porphyry and gabro. | J           | J  |

Table 2: Summary of aquifer parameters of the PTA (adapted from JICA-DGA-PCI, 1995)

| Zone                            | Transmissivity<br>[m <sup>2</sup> /d] | Hydraulic Conductivity<br>[m/d] | Storativity<br>[ - ] |
|---------------------------------|---------------------------------------|---------------------------------|----------------------|
| Dolores                         | 1 – 1031                              | 0.02 – 101.1                    | 3e-04 – 0.05         |
| Huara                           | 8 – 1506                              | 0.11 – 20.3                     | 5.7e-07 – 0.08       |
| Pozo Almonte<br>Pintados        | 9 – 1094                              | 0.3 – 91.6                      | 9.4e-06 – 0.04       |
| Oficina Victoria<br>Cerro Gordo | 81 – 420                              | 0.8 – 12                        | 3e-07 – 0.33         |

Table 3: Estimation of recharge (l/s) for PTA (After JICA-DGA-PCI, 1995)

| Location                    | Recharge [l/s] |
|-----------------------------|----------------|
| <i>Aroma</i> sub-basin      | 310            |
| <i>Tarapaca</i> sub-basin   | 318            |
| <i>Sagasca</i> sub-basin    | 89             |
| <i>Quipisca</i> sub-basin   | 72             |
| <i>Quisma</i> sub-basin     | 21             |
| <i>Chacarilla</i> sub-basin | 159            |
| <i>Ramada</i> sub-basin     | 7              |
| Total Recharge              | 976            |

Table 4: Annual transpiration demands (l/s) for the *Tamarugo* zones in the study area  
(adapted from DGA-UChile, 1988 and JICA-DGA-PCI, 1995)

| Year      | Transpiration [l/s] |
|-----------|---------------------|
| 1960      | 210                 |
| 1980-1985 | 690                 |
| 1985-1993 | 904                 |

Table 5: Water balance (l/s) for years 1960, 1987, 1993

| Flow Components                     | 1960       |            | 1987       |                  | 1993       |                  |
|-------------------------------------|------------|------------|------------|------------------|------------|------------------|
|                                     | In         | Out        | In         | Out              | In         | Out              |
| Recharge from sub-basins            | 976        |            | 976        |                  | 976        |                  |
| Transpiration <i>Tamarugo</i> areas |            | 210        |            | 690              |            | 904              |
| Evaporation from <i>Salares</i>     |            | 410-602    |            | 286              |            | 145              |
| Groundwater Outflow                 |            | 164-356    |            | 164-356          |            | 164-356          |
| Pumping Discharge                   |            | 0          |            | 716              |            | 730              |
| <b>TOTAL</b>                        | <b>976</b> | <b>976</b> | <b>976</b> | <b>1856-2048</b> | <b>976</b> | <b>1943-2135</b> |

Table 6: Simulated water balance results (l/s) for years 1960, 1987, 1993

| Flow Components                     | 1960       |            | 1987       |             | 1993       |             |
|-------------------------------------|------------|------------|------------|-------------|------------|-------------|
|                                     | In         | Out        | In         | Out         | In         | Out         |
| Recharge from sub-basins            | 976        |            | 976        |             | 976        |             |
| Transpiration <i>Tamarugo</i> areas |            | 210        |            | 676         |            | 890         |
| Evaporation from <i>Salares</i>     |            | 603        |            | 362         |            | 275         |
| Groundwater Outflow                 |            | 163        |            | 156         |            | 170         |
| Pumping Discharge                   |            | 0          |            | 716         |            | 730         |
| <b>TOTAL</b>                        | <b>976</b> | <b>976</b> | <b>976</b> | <b>1910</b> | <b>976</b> | <b>2065</b> |

## List of Figures

- Fig. 1: Location of the study area. a) General location, b) Aquifer and sub-basins delimitation, c) Observation wells in the study area
- Fig. 2: Geological longitudinal profile (X1 – X'1) of PTA- white dashed lines indicating main faults - (adapted from JICA-DGA-PCI, 1995)
- Fig. 3: Observed groundwater heads in Wells (30) and (72) - depth in meters below ground level [m b.g.l.] and head in meters above sea level [m a.s.l.]
- Fig. 4: Equipotential map for the PTA in the year 1960 (adapted from JICA-DGA-PCI, 1995)
- Fig. 5: Artificial groundwater discharge in the study area
- Fig. 6: Observed vs. simulated groundwater heads: a) steady-state for the year 1960, b) transient-state for the period (1983-2004)
- Fig. 7: Spatial distribution of error terms for steady-state model
- Fig. 8: Observed and simulated groundwater heads in time: a) *Well Dolores* (North Sector), b) *Well 60-59* (Centre-North Sector), c) *Well 134* (Centre-Centre Sector), d) *Well 31* (Centre-South Sector), e) *Well 276* (South Sector)
- Fig. 9: Annual simulated flow components for scenarios 2005, 2005+20%, 2005-20% and *DWP*: a) evaporation flow rates (l/s) from salares, b) groundwater flow to storage (l/s), and c) loss of groundwater storage (l/s)
- Fig. 10: Results for random recharge flow rates generation: a) Annual loss of groundwater storage for  $\sigma_3$  and for 100 recharge realizations, b) Average loss of groundwater storage vs. number of realization for three uncertainty levels for the year 2050, c) Standard deviation of the loss of groundwater storage vs. number of realization for three uncertainty levels for the year 2050, d) Probability distribution for the simulated cumulative loss of groundwater storage for  $\sigma_3$  for the year 2050
- Fig. 11: Simulated groundwater heads for a synthetic observation well in the *Aroma* creek for  $\sigma_3=0.35R$  and for 100 recharge realizations (the black line represents the average recharge value)

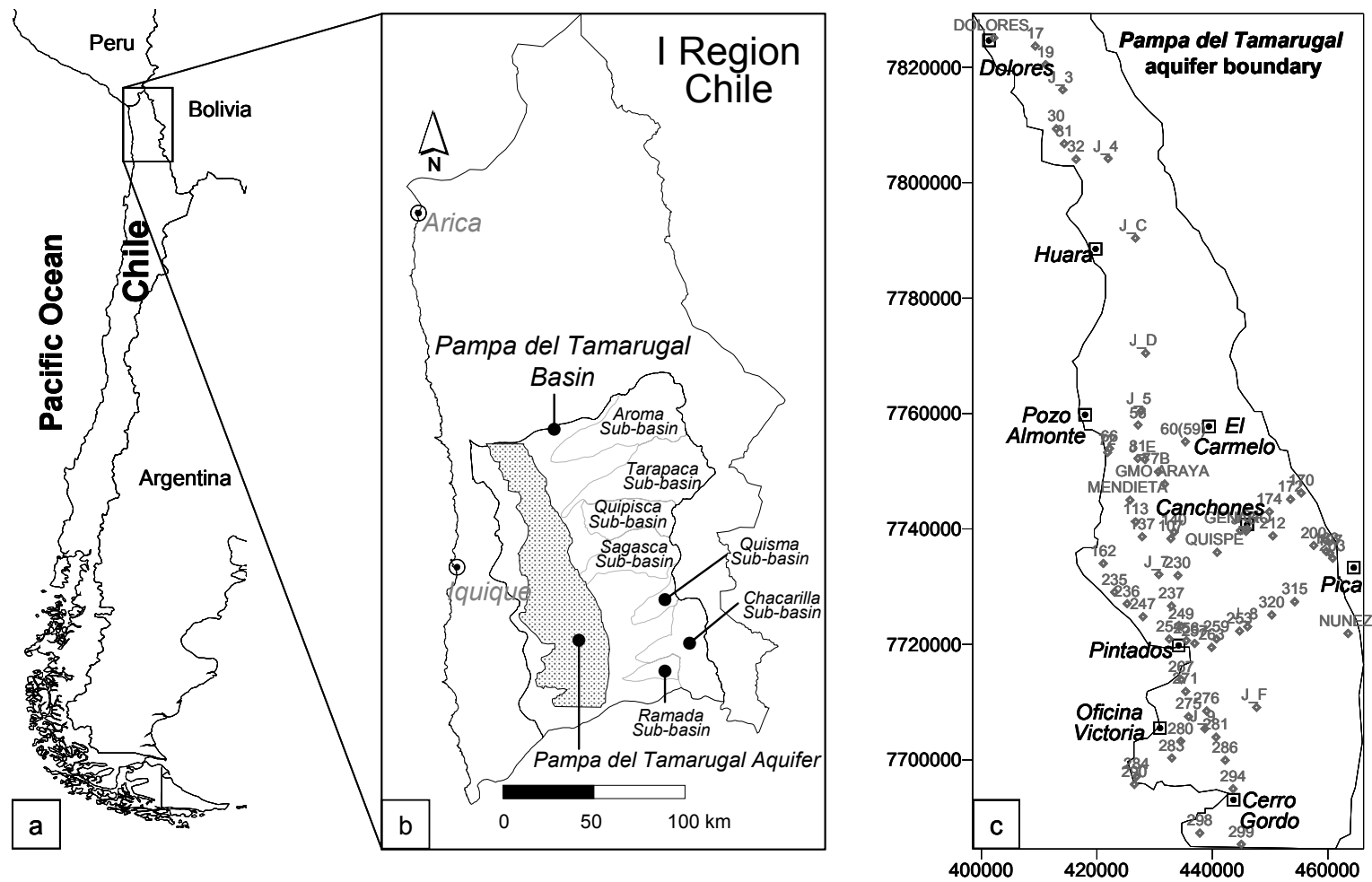


Fig. 1: Location of the study area. a) General location, b) Aquifer and sub-basins delimitation, c) Observation wells in the study area



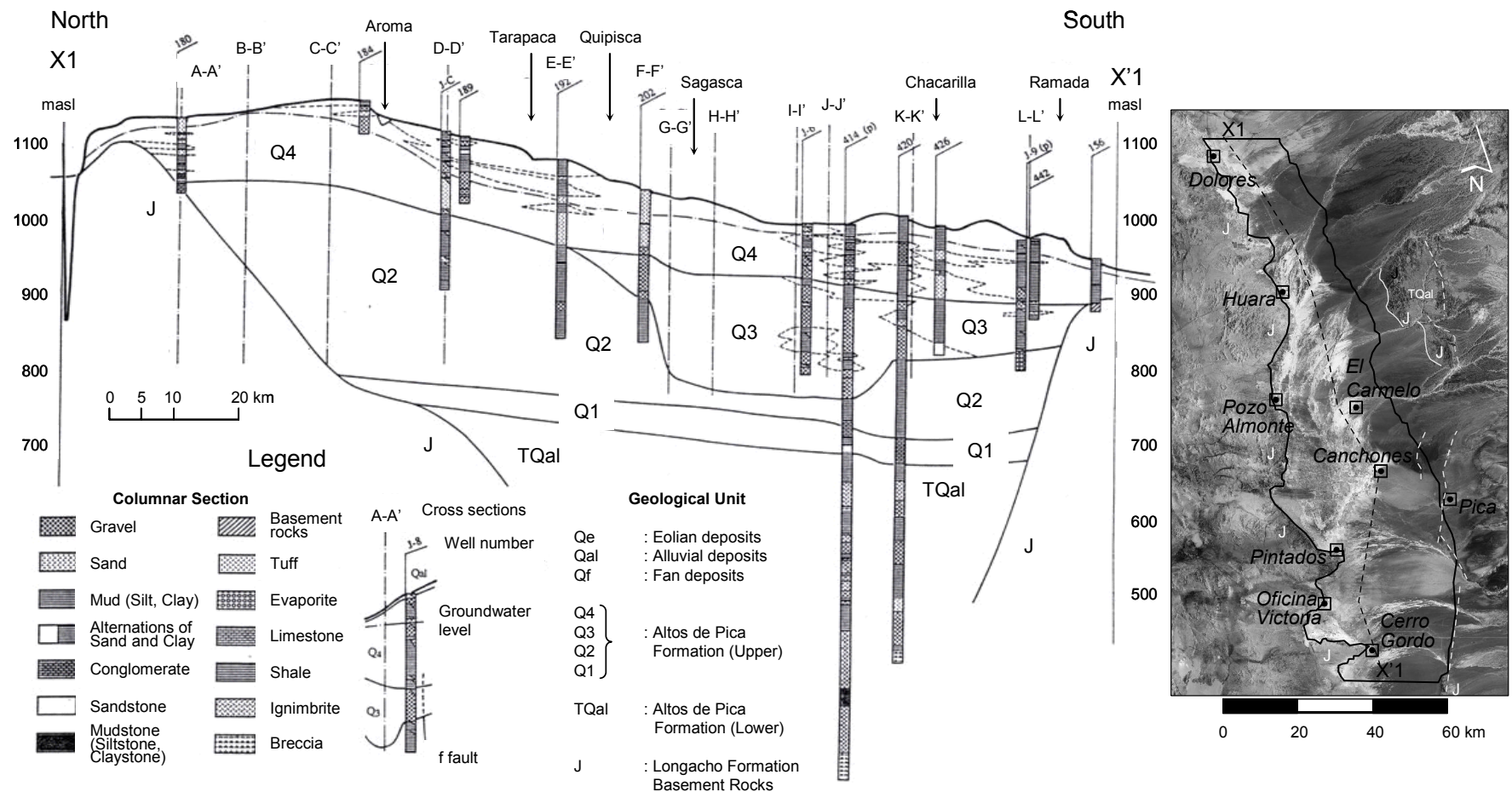


Fig. 2: Geological longitudinal profile (X1 – X'1) of PTA- white dashed lines indicating main faults - (adapted from JICA-DGA-PCI, 1995)

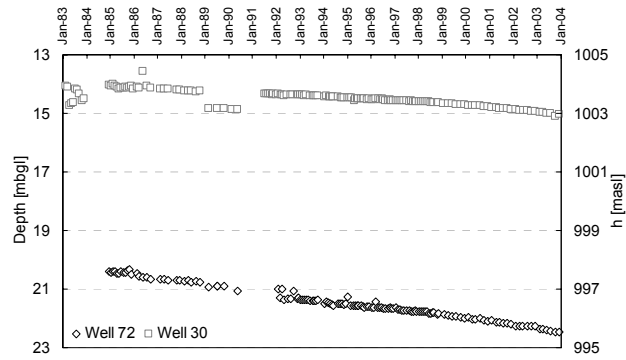


Fig. 3: Observed groundwater heads in Wells (30) and (72) - depth in meters below ground level [m b.g.l.] and head in meters above sea level [m a.s.l.]

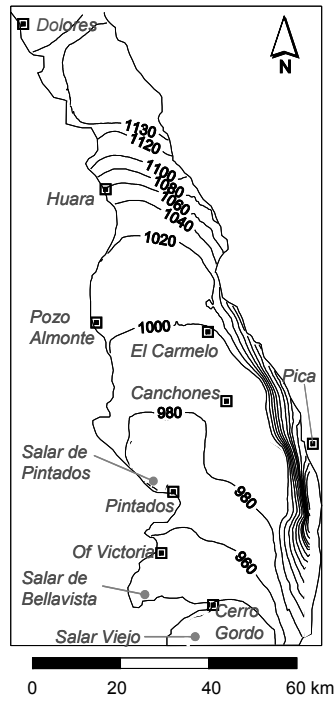


Fig. 4: Equipotential map for the PTA in the year 1960 (adapted from JICA-DGA-PCI, 1995)

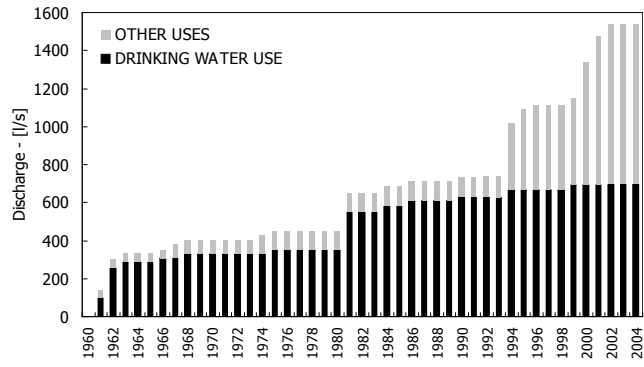


Fig. 5: Artificial groundwater discharge in the study area

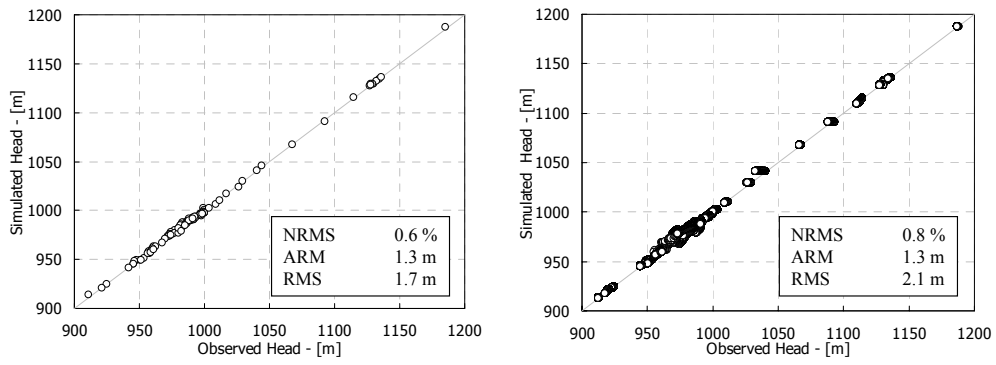


Fig. 6: Observed vs. simulated groundwater heads: a) steady-state for the year 1960, b) transient-state for the period (1983-2004)

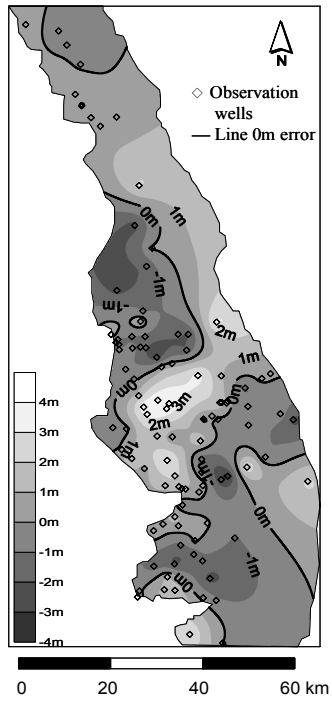


Fig. 7: Spatial distribution of error terms for steady-state model

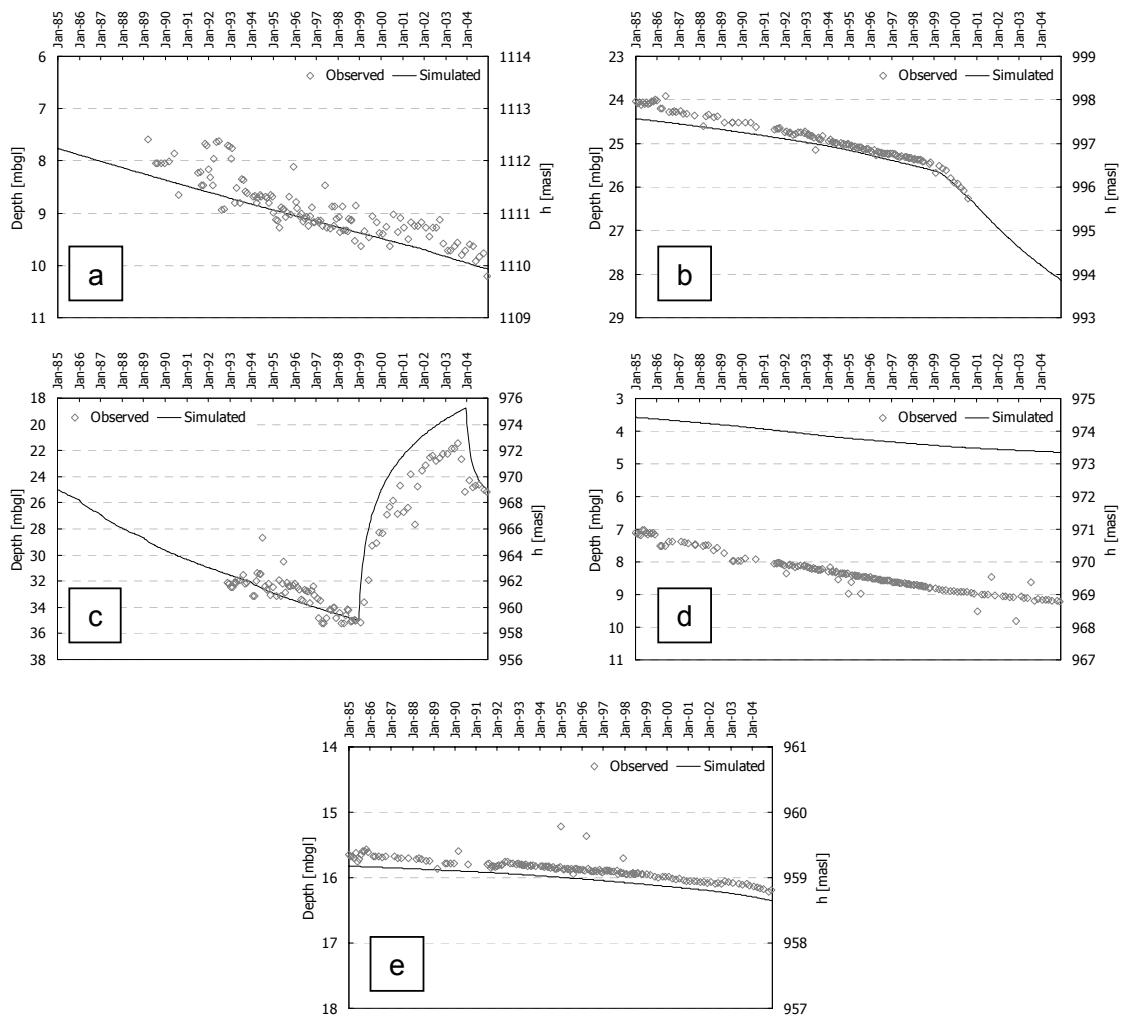


Fig. 8: Observed and simulated groundwater heads in time: a) *Well Dolores* (North Sector), b) *Well 60-59* (Centre-North Sector), c) *Well 134* (Centre-Centre Sector), d) *Well 31* (Centre-South Sector), e) *Well 276* (South Sector)

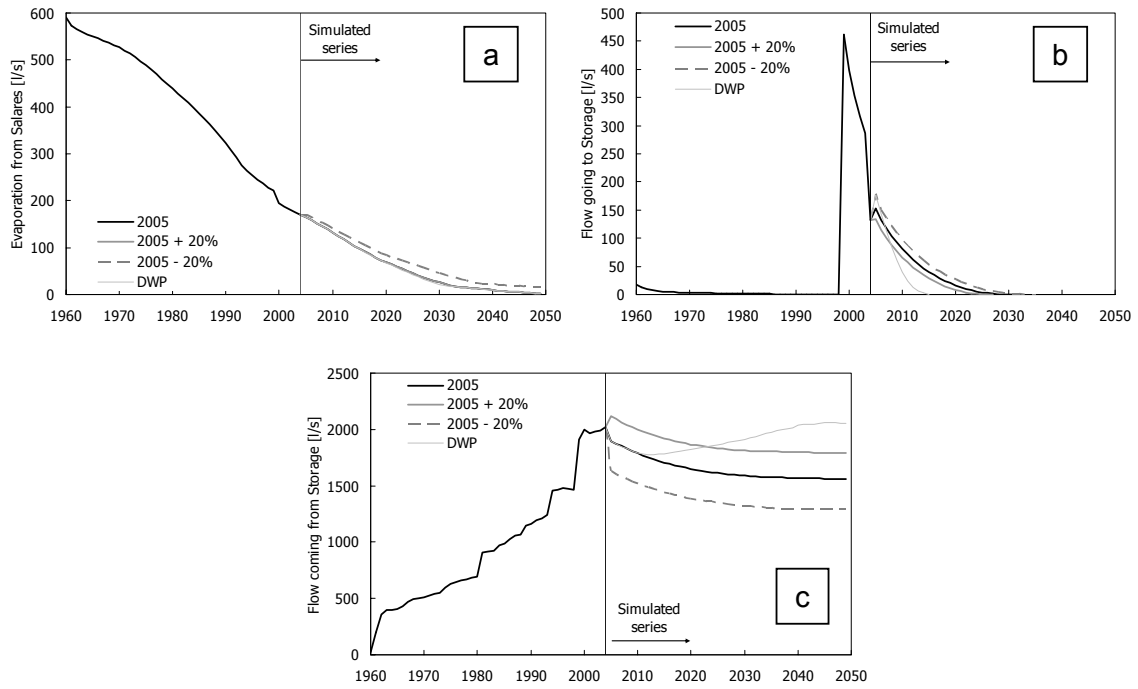


Fig. 9: Yearly simulated flow components for scenarios *2005*, *2005+20%*, *2005-20%* and *DWP*: a) evaporation flow rates (l/s) from salares, b) groundwater flow to storage (l/s), and c) loss of groundwater storage (l/s)



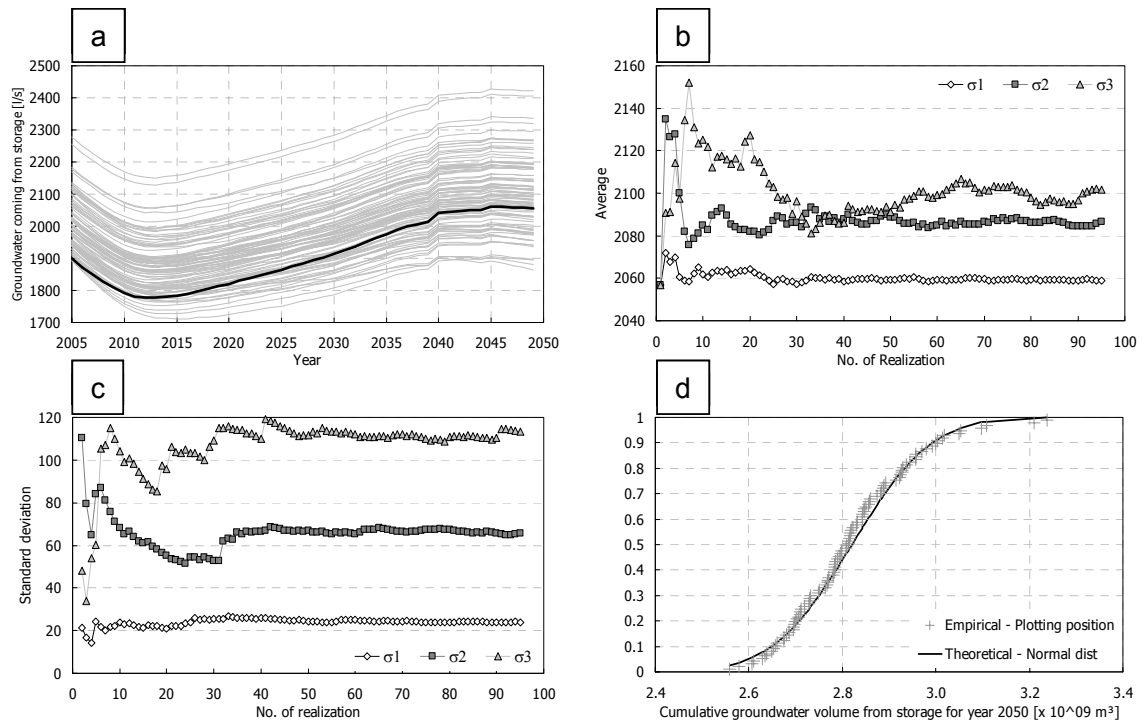


Fig. 10: Results for random recharge flow rates generation: a) Annual loss of groundwater storage for  $\sigma_3$  and for 100 recharge realizations, b) Average loss of groundwater storage vs. number of realization for three uncertainty levels for the year 2050, c) Standard deviation of the loss of groundwater storage vs. number of realization for three uncertainty levels for the year 2050, d) Probability distribution for the simulated cumulative loss of groundwater storage for  $\sigma_3$  for the year 2050

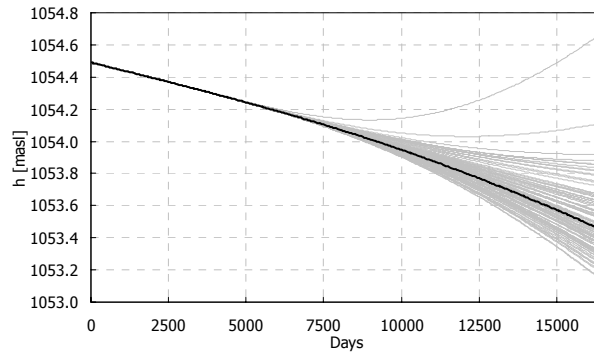


Fig. 11: Simulated groundwater heads for a synthetic observation well in the *Aroma* creek for  $\sigma_3=0.35R$  and for 100 recharge realizations (the black line represents the average recharge value)